J Chem Biol (2009) 2:161–175
DOI 10.1007/s12154-009-0024-8

REVIEW

Fluorescent oligo and poly-thiophenes and their utilization for recording biological events of diverse origin—when organic chemistry meets biology

Andreas Åslund · K. Peter R. Nilsson · Peter Konradsson

Received: 30 April 2009 / Accepted: 29 June 2009 / Published online: 2 August 2009

Abstract The technique of using luminescent oligo-thiophenes and luminescent conjugated poly-thiophenes to monitor biological processes has gained increased interest from scientists within different research areas, ranging from organic chemistry and photo-physics to biology since its introduction. The technique is generally straightforward and requires only standard equipment, and the result is available within minutes from sample preparation. In this review, the syntheses of oligo and polythiophenes developed over the last decades are discussed. Furthermore, the utilization of these molecular agents for exploring biological events, e.g., DNA hybridization or protein misfolding events, are covered.

Keywords Polythiophene · Oligothiophene · DNA hybridization · Amyloid · Prion

Introduction

This review will focus on two aspects of luminescent oligo-thiophenes (LCOs) and luminescent conjugated poly-thiophenes (LCPs). In part one, different ways to prepare LCOs and LCPs and how the synthetic methods have progressed over time will be discussed. We will not cover mechanistic aspects in detail or elaborate further every variation of the methods used. However, our goal is to provide the reader with a comprehensive overview of the synthetic routes that have been published in the area, based on what we feel are the most important synthetic leaps forward. In the second part, we will cover how the optical properties of LCOs and LCPs have been utilized for recording molecular events, such as DNA hybridization and protein folding/misfolding in biological systems.

Over the last decade, we have spent a great deal of time and effort preparing and characterizing LCPs, en route for studying biological systems and events. These materials have over and over again surprised us with the selectivity and specificity with which they can visualize, mainly via fluorescence, various biological events in vitro. The interest for LCPs started off with a serine functionalized LCP (Fig. 4e) [1], originally synthesized for use in electrical devices. It was realized that upon dissolution in different buffers, the wavelength of the light absorbed and emitted by the polymer changed [2]. Inspired by the work of Bednarsky et al. [3], Ewbank et al. [4], and Barbarella et al. [5], the idea of using the serine functionalized LCP in biological systems spawned, and later, it was shown that DNA hybridization events could be followed by fluorescence [6]. Moreover, it was shown that the conformation-sensitive properties of POWT allowed visualization of the structural change from a random coil structure of the synthetic peptides JR2E and JR2K alone in solution to a four-bundle helix motif when the two peptides were mixed together [7]. Later, LCOs and LCPs have shown a unique potential as a research tool especially within protein misfolding-associated events and diseases.

A. Åslund · K. P. R. Nilsson · P. Konradsson
Department of Physics, Chemistry and Biology,
Linköping University,
Linköping, Sweden

A. Åslund (✉)
Linköpings Universitet,
IFM-Kemi, Valla Hus B,
581 83 Linköping, Sweden
e-mail: andas@ifm.liu.se

Synthesis

Even though the synthesis of a bithiophene was reported as early as 1894 [8], the polymerization of thiophene was not carried out until 1980 when two groups independently described the polymerization of 2,5-dibromothiophene using the Kumada coupling of Grignard reagents into polythiophenes (Fig. 1a) [9, 10]. Another polymerization method, introduced by Sugimoto and coworkers in 1984, was iron(III)chloride ($FeCl_3$)-mediated and carried out in chloroform (Fig. 1b) [11]; the reaction takes place on the surface of the insoluble $FeCl_3$ and has become the method of choice for the synthesis of LCPs used for fluorescence detection of viruses [12], DNA hybridization [6, 13], and protein folding and misfolding events [7, 14–19]. This reaction was recently modified in our lab to be carried out in an aqueous solution with a catalytic amount of $FeCl_3$ and $Na_2S_2O_8$ as the primary oxidant (Fig. 1d) [20]. This ensures low content of iron impurities that could interfere in biological measurements, e.g., by being toxic as well as in electronic applications by reducing the charge transfer properties by unintentional doping from the metal ion [20].

One drawback of polymerization is the variations that inherently are a part of the material. If one polymerizes an unsymmetrical starting material, the product polymer will be regio-irregular, that is, it consists of a mixture of head to tail (HT), head to head (HH), and tail to tail (TT) coupled monomers (Fig. 1c). Moreover, the material will have a distribution of different chain lengths, and in the case of $FeCl_3$ polymerization, chloride termination of the α-position of the polythiophene is a known side reaction [16, 17, 21, 22]. Furthermore, the characterization of the material is cumbersome. The use of size exclusion chromatography is a common way of determining the size

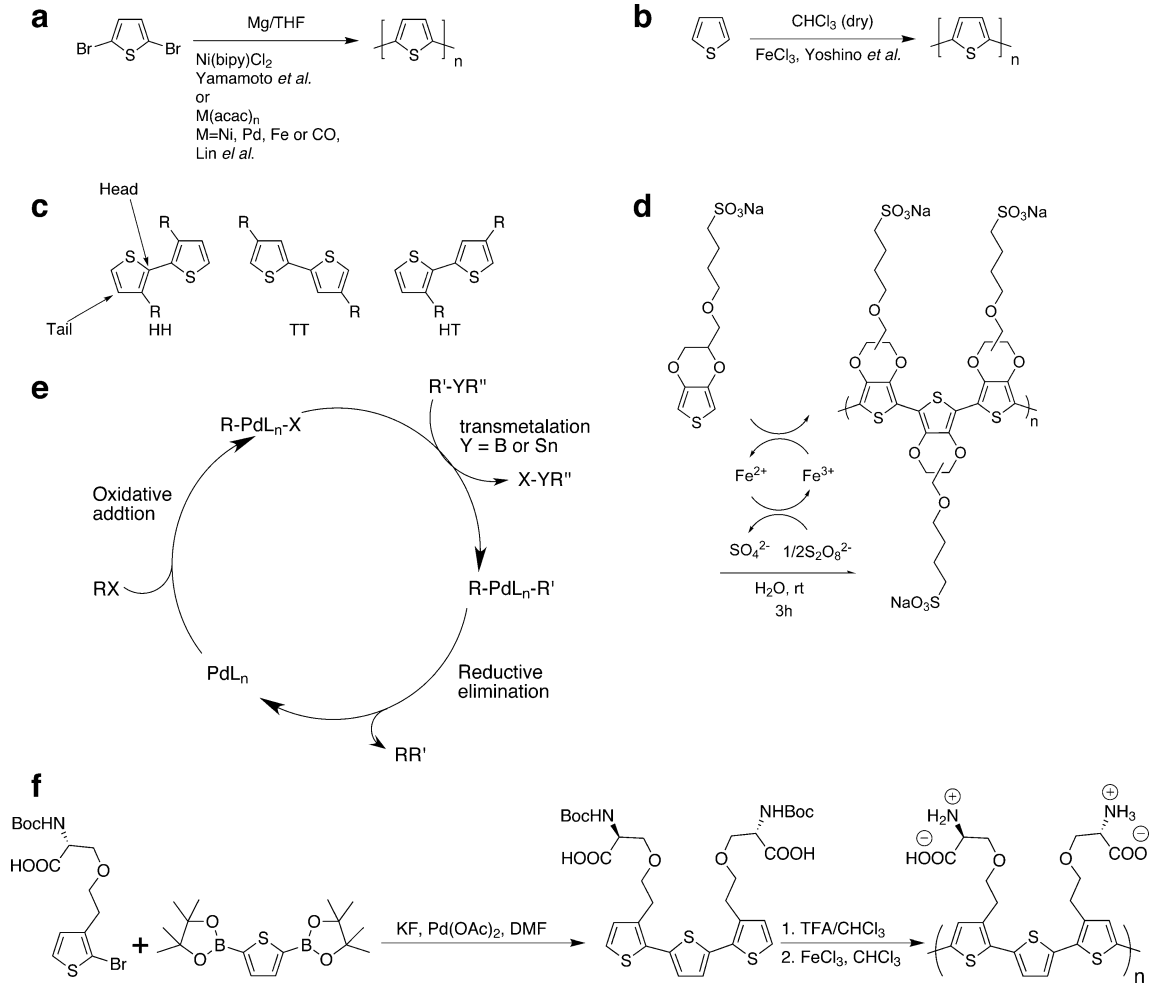

Fig. 1 **a**, **b** Different polymerization methods. **c** Different configurations of thiophenes; head to head (*HH*), tail to tail (*TT*), and head to tail (*HT*). **d** Polymerization reaction using a catalytic amount of $FeCl_3$. **e** General catalytic cycle for Stille and Suzuki cross coupling reactions. **f** Synthesis of a regio-regular polythiophene

distribution of polymers. However, the polystyrene standard used to calibrate for size has very different geometrical restraints compared to LCPs; therefore, the absolute size of the polymer chains can differ from the measured value [23, 24]. Another common way to determine the size and distribution of LCPs is matrix-assisted laser desorption/ionization-time of flight mass spectrometry (MALDI-TOF MS), though this technique also has its drawbacks. Firstly, not all LCPs can be ionized, whereby the technique is of no use. Secondly, care is required when one interprets the acquired data, since the masses found on MALDI-TOF MS do not always give a true picture of the actual chain length distribution due to the diverse readiness of ionization of chains of different lengths [25].

The regio-irregularity problem has been overcome in several ways. In 1992, McCullough and Lowe used Kumada coupling to get quantitative HT coupling (Fig. 1f) [26]. Leclerc and coworkers have polymerized 3-alkoxy-4-methylthiophene in $FeCl_3$ and shown that the sterically less congested alkoxy group, compared to the methyl group, will favor HT coupling [19]. An alternative solution to the problem is to couple two unsymmetrical monomers under controlled conditions into a symmetrical thiophene dimer. Upon polymerization, this results in a regio-regular HH–TT polymer [27]. A different approach would be to couple two unsymmetrical monomers to a third symmetrical unit schematically depicted in Fig. 1. A more comprehensive summary of different polymerization methods of thiophene derivatives can be found in a review written by Richard D. McCullough [28]. Regarding problems with regio-irregularity, McCullough and Osaka published a review in 2008 [29].

The availability of easily accessible materials that are chemically defined and well characterized is crucial when one wants to go into molecular detail of the binding events of LCPs or LCOs in biological systems. Today, variations of the Stille [30] and Suzuki [31, 32] cross-coupling reaction of vinylic and aromatic compounds are the two most common ways to overcome the obstacles that polymerization present, although they, too, can be used for polymerization. Both are palladium-catalyzed reactions based on similar catalytic cycles consisting of three steps, oxidative addition, transmetalation, and reductive elimination (Fig. 1e). The Stille reaction couples halogen and stannyl compounds whereas the Suzuki reaction couples halogen and boronic acid or ester derivatives in the presence of base. The role of the base is to facilitate the transmetalation by activating the boron, but the exact mechanism remains unclear. The properties of the catalyst need to be tuned for all three steps to be effective. In the oxidative addition of the halogenated species, the catalyst is the nucleofile and is preferably electron-rich; however, the transmetalation requires an electron-deficient metal for the nucleofilic stannyl or boronyl to attack the planar tetrahedral metal center of the catalyst. Moreover, steric hindrance is thought to favor the reductive elimination [33]. Farina et al. [33] has studied the rate dependence of the palladium catalyst ligand in the Stille cross-coupling and found that the most commonly used ligand, triphenylphospine (PPh_3), was not at all the best ligand. Using tri-2-furylphosphine and triphenylarsine, 105 and 1,100 times higher rates, respectively, and excellent yields compared to PPh_3 [33] were achieved. Typically, the exact cross-coupling conditions have to be determined for each individual reaction. The necessity of a base in the Suzuki coupling adds a parameter that can be varied, and finding the good reaction conditions may often be time consuming. This has led not only to the development of a variety of phosphine ligands vide supra but also to the search for alternatives to the phosphine/arsine ligands. The most promising ligands today are the *N*-heterocyclic carbene (NHC)-based ones. Herrmann et al. were the first to propose the NHCs as spectator ligands in transition-metal complexes [34], and since then, the development towards air-stable promiscuous metal-NHC catalysts have made an impact in transition metal cross-coupling reactions. In a phosphine ligand, the steric substituents are directly attached to the donor atom; therefore, the electronic and sterical properties of the ligand that are important at different stages of the catalytic cycle are not easily separated. With NHCs, on the other hand, the steric bulk of the ligand is not directly coupled to the carbene; therefore, they can be independently tuned to obtain selectivity and good yields [35]. When electron-rich species such as thiophenes or pyrroles are coupled, the Stille reaction generally works better than the Suzuki reaction [36]. McCoullugh et al. used a CuO-modified Stille cross-coupling for the polymerization of thiophene depicted in Fig. 2a [4]. The same year, 2001, Barbarella et al. reported the first synthesis of a LCO using the Stille reaction in 70 % yield (Fig. 2b) [5].

Even though the Stille reaction is an excellent method to make carbon–carbon bonds between aromatic compounds, the negative environmental and health risks that involve working with tin have shifted attention towards the Suzuki reaction. A common side-reaction of the Suzuki cross-coupling reaction is homo-coupling of the boronic acid or ester [37]; this is normally circumvented by using the more stable boronic esters over boronic acid and by adding an excess of the boronic ester. The Suzuki reaction can be carried out in various solvents including water and ethanol, and the boronic acid and ester are generally stable under ambient conditions. Furthermore, boronyl derivatives are commercially more available than stannyl derivatives.

To the best of our knowledge, Bäuerle and coworkers were the first to utilize Suzuki cross-coupling-like conditions for a thiophene–thiophene coupling in 1999

(Fig. 2c) [38]. In 2000, they showed a feasible route to synthesize LCOs using hydroxymethyl polystyrene resin containing a silyl linker in eight consecutive steps with an overall yield of 48% of which three were Suzuki cross-coupling reactions (the last steps are shown in Fig. 2d) [39]. In the same year, they published another route to LCOs using a chloromethylated polystyrene resin with a carboxylic acid linker (the last steps are shown in Fig. 2e) [40]. The difference in linkers resulted in two different LCOs, since the silyl linker was completely removed from the LCO upon cleavage from the resin, whereas the carboxylic acid linker remained on the thiophene after cleavage and, therefore, can be used for further modification of the LCO. Bäuerle and coworkers have later shown how thiophene activation with iodine and bromine can be used to selectively cross-couple the iodine-activated site and a boronic ester to a HT dimer, while the bromine activated site is left unreacted for later use (Fig. 2f) [41]. Often the LCOs wanted for a special application are of hydrophobic nature, which rule out environmentally friendly solvents such as water or ethanol. This has led to the development of cross-coupling methods under solvent-free conditions [37, 42]. The reaction took place on Al_2O_3 and after the reaction, the crude product could be rinsed off and boron salts and catalyst were left on the aluminum oxide (Fig. 2g). Furthermore, they also showed how two brominated thiophenes could be coupled in the presence of bis (pinacolato)diboron that generated the thiopheneboronic ester in situ (Fig. 2g).

The use of a NHC-based catalyst in the synthesis of LCPs was first reported in 2007 [17, 18], where it was used to make a thiophene trimer building block (Fig. 2h) that was later polymerized by the method described by Sugimoto and coworkers [11]. The catalyst was the commercially available PEPPSI-IPr (Fig. 2i) [43] used under microwave conditions. The necessity to keep the ratio of the boronic ester at the highest 0.5 equivalents makes this particular coupling somewhat demanding due to the risk of homo coupling previously mentioned. In this particular coupling, it is not possible to use an excess boronyl owing to the risk of ending up with a large part of mono-coupled bithiophene. It was not desirable to perform the coupling as it was described by Herland et al. (Fig. 1f) [16]. Instead, the amino acid was introduced at a later stage of the synthesis, giving rise to a more divergent route to differently functionalized LCPs and LCOs. Furthermore, one reason for the somewhat low yield of 36% percent in the coupling Herland et al. reported has later been attributed to hydrolyzation of the ether side chain when $Pd(OAc)_2$ was the catalyst. When PEPPSI-IPr was tried in the same reaction, the hydrolyzation was quantitative (Åslund A, unpublished results). However, the NHC-Pd catalyst increased the yield of the coupling to 66% if the coupling was performed before the serine functionalization. Since then, the reaction has been further optimized and the thiophene-diboronic acid pinacol ester has been replaced with the commercially available thiophene-diboronic acid, the halogen has been changed from iodine to bromine, and the reaction temperature has been lowered from 100°C to 80°C, while the yield has been raised to an acceptable 88 % (Fig. 2h; Åslund A, unpublished results).

LCOs and LCPs recording biological events

The focus on conjugated polymers has, since the 1970s, been on utilizing these materials in electronic devices such as solar cells and displays; the importance of this was accentuated when the Nobel prize was awarded to Alan J Heeger, Alan G. MacDiarmid, and Hideki Shirakawa in 2000 “for the discovery and development of conductive polymers”. However, conjugated polymers, especially polythiophenes and polyfluorenes, also exhibit interesting intrinsic optical properties that can be correlated to the geometry of the polymer backbone. These optical properties have been used to record biological events and to our knowledge, the proof of principle was first shown by Bednarski and coworkers in 1993 [3]. They used a ligand-functionalized conjugated polymer (polydiacetylene) to monitor a ligand–receptor interaction by the colorimetric change in the coil-to-rod transition of the polymer. Analyte specificity in this first generation of conjugated polymer-based biosensors was due to the covalent integration of ligands on the side chains of the conjugated polymers. Hence, the detection and recognition event was a function of the nature and characteristics of the side chains. However, this is a major drawback as the side chain functionalization of the conjugated polymer requires advanced synthesis and extensive purification of numerous monomeric and polymeric derivatives. Secondly, this first generation of sensors mainly used optical absorption as the source for detection, and the sensitivity of these sensors was much lower compared with other sensing systems for biological events. To avoid covalent attachment of the receptor to the polymer side chain and to increase the sensitivity of the biosensors, LCPs and LCOs have been utilized.

The physical properties of an ideal fluorophore ought to have high absorbance, high quantum yield, and big Stokes shift separating the absorption and emission spectra [5]. Furthermore, to diminish background fluorescence, the excitation and emission of the probe should be in the visible or near-infrared spectra and be both specific and selective. The probe should be resistant to photobleaching and photoactivation, and a “turn on” of the fluorescence signal upon interaction is preferred over a “turn off” [44]. If the LCO/LCP is intended for in vivo or

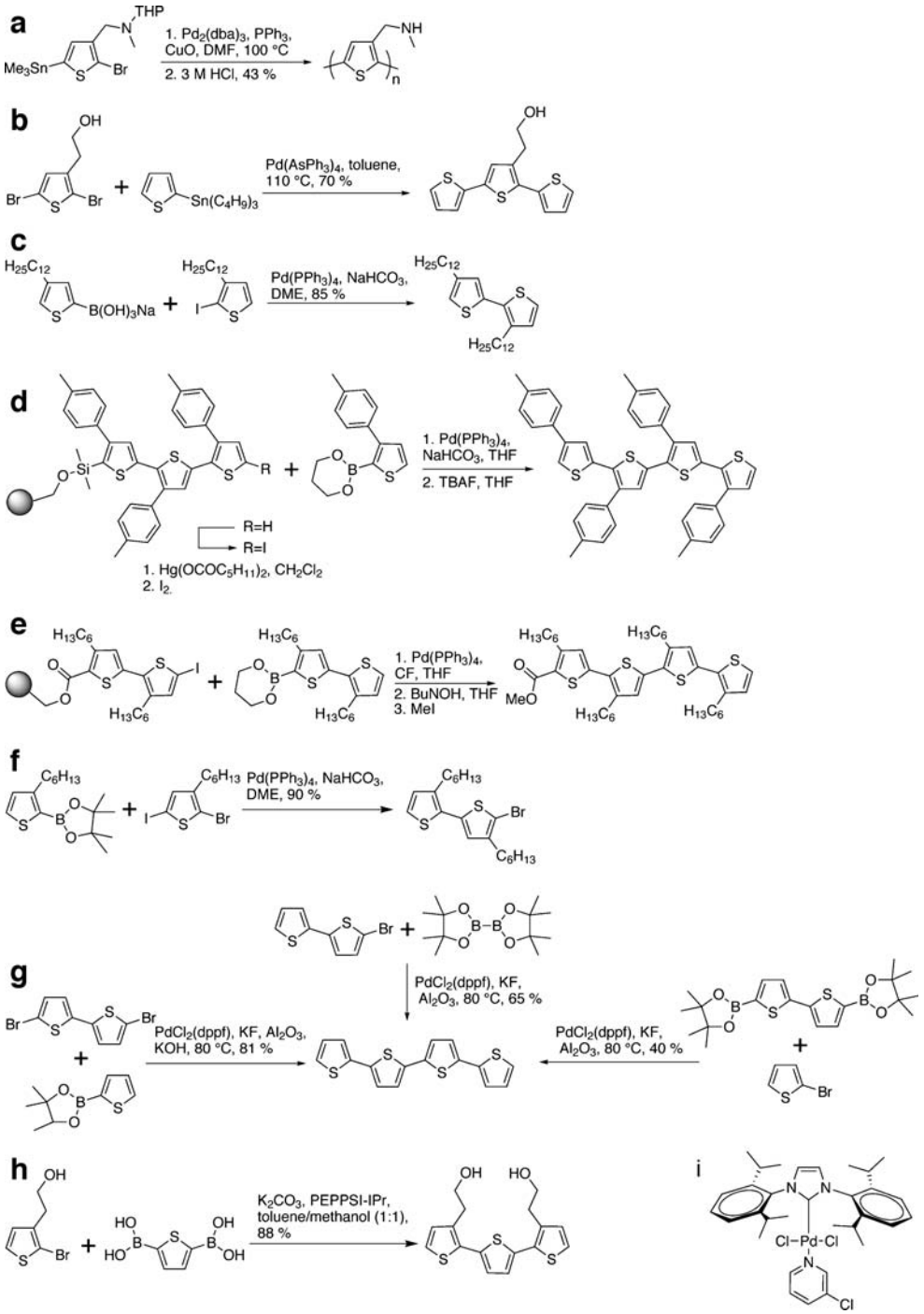

Fig. 2 **a**–**h** Different uses of the Stille and Suzuki cross-coupling reactions. **i** The commercially available cross-coupling catalyst PEPPSI-IPr, [1,3-Bis(2,6-Diisopropylphenyl)imidazol-2-ylidene](3-chloropyridyl)palladium(II) dichloride

live cell staining, it should also have low or preferably no toxicity at the administered dose and be stable and soluble under physiological conditions. One feature LCOs and LCPs have, in contrast to the traditional stiff small molecular dyes, is a flexible backbone (Fig. 3a). This means that the backbone of the LCOs/LCPs can adopt different geometrical shapes and if the backbone becomes conformationally restricted, for instance due to the interaction with a biological target, this will affect the fluorescence from the dye. A twist of the backbone gives rise, as a result of shorter effective conjugation length, to a blue shift; whereas flattening of the

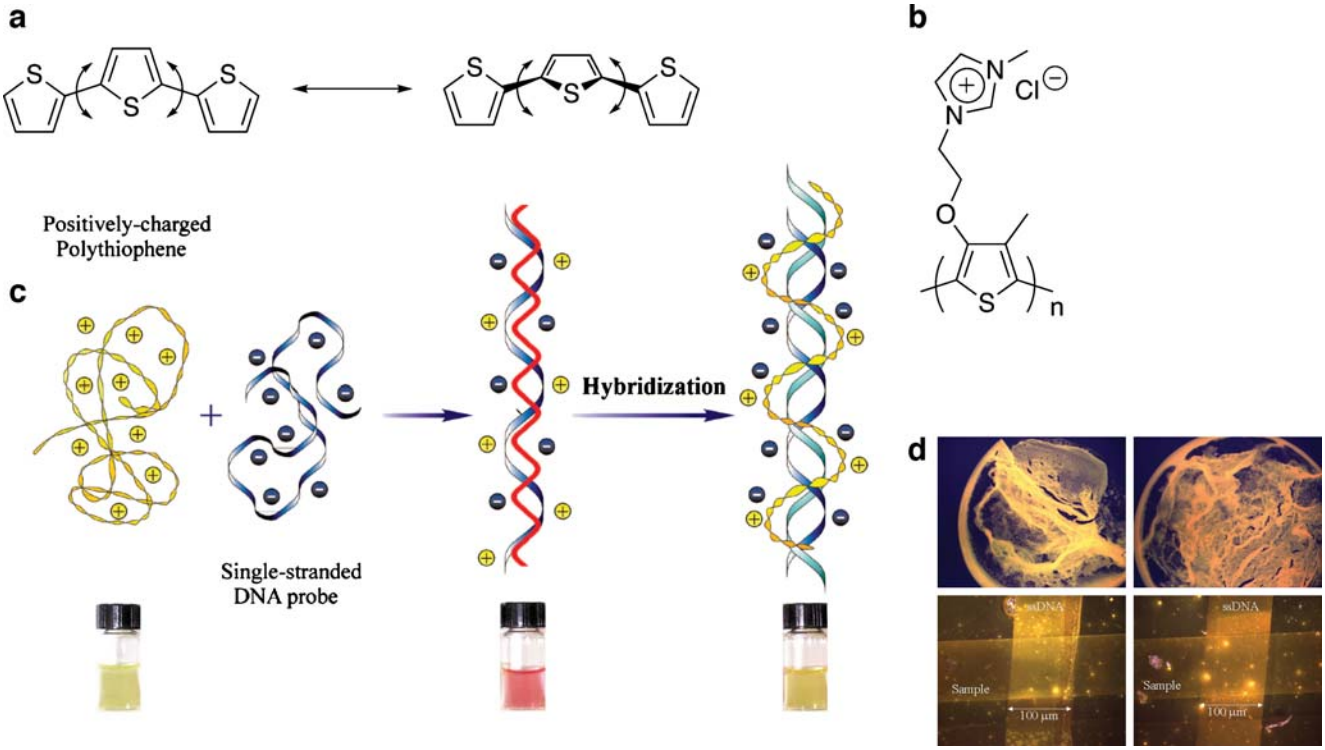

Fig. 3 **a** Twisting of the LCO/LCP backbone. **b** Cationic LCP. **c** Depiction of the detection scheme for DNA. *Left*, before LCP-ssDNA interaction the LCP is yellow. *Middle*, LCP-ssDNA interaction, the LCP is in a planar configuration seen as a red color. *Right*, LCP-dsDNA interaction, the LCP is twisted in its configuration seen as a yellow color. **d** Fluorescence images of POWT (Fig. 4e)/DNA complexes. Hydrogels of POWT and ssDNA after binding of complementary DNA (*upper left*) and non-complementary DNA (*upper right*). Cross points (100 Å~ 100 μm) of POWT and ssDNA after binding of complementary DNA (*lower left*) or non-complementary DNA (*lower right*). Subpanel **c** is reprinted with permission from [52]. ©2008 *American Chemical Society*. Subpanel **d** is adapted by permission from Macmillan Publishers Ltd: *Nature Materials*, ©2003 [6]

backbone increases the effective conjugation, which results in a red shift [45]. The optical transitions of the LCO/LCP are also governed by stacking between thiophene rings on adjacent polymer chains. In this case, intermolecular radiative and non-radiative relaxation pathways occur more frequently and the spectral changes in the form of red shift and lowered quantum efficiency is a result thereof.

Other non-thiophene-based luminescent conjugated polymers have been used rather extensively to study biological events [44–54]. These systems utilize the excellent light-harvesting properties of conjugated polymers instead of the intrinsic conformationally induced optical properties, as the detection schemes for studying the biological events are mainly based on quenching of the emission from the polymer or fluorescence resonance energy transfer (FRET) between the polymer and a second fluorophore. Although these molecules have been successfully employed for recording DNA-hybridization events as well as protein interactions [46–50], the following sections will focus on LCPs and LCOs, as the thiophene based molecules have been proven useful for studying a greater diversity of biological events.

LCPs for recording DNA-hybridization events

The concept of utilizing a LCP as DNA sequence specific marker was first shown by Leclerc and coworkers [13, 51]. By using a cationic LCP (Fig. 3b), they nicely showed how the flexibility of the thiophene backbone can be utilized for detection of hybridized, double-stranded DNA (dsDNA). When the LCP was free in solution, it had an absorbance maximum of 397 nm corresponding to a twisted conformation. Upon mixing with the negatively charged single-stranded DNA (ssDNA) oligonucleotide, A-1, the electrostatic interaction between the LCP and A-1 oligonucleotide red-shifted the absorption maximum from 130 to 527 nm, corresponding to a planarization of the backbone. The optical transition could easily be seen by the naked eye as the color of the solution changed from yellow to red (Fig. 3c). When a complementary oligonucleotide (B-2) strain was added to the first complex, a double-stranded oligonucleotide was formed, and the solution turned yellow, as the LCP once again was in its twisted configuration. However, the LCP was still in conjunction with the A-1/B-1 complex as circular dichroism (CD) revealed a bisignate spectra at

420 nm, characteristic of a right-handed twisted helical LCP structure. The LCP alone in solution or in complex with the ssDNA did not reveal any chirality. The detection limit was as low as 3×10^6 molecules in 200 μL solution. The robustness of the technique was verified with the complementary oligonucleotide B-2 and B-3 with two and one base pair mismatch each, respectively. In these cases, a perfect dsDNA strand did not form, and the red-shifted spectra were retained with minor alterations.

Later, Leclerc and coworkers modified the system by covalently attaching a chromophore (Alexa Flour 546) to the oligonucleotide, forming an A-1-Alexa complex [52]. The idea was to use FRET, where the added chromophore served as an acceptor, and the LCP was the donor. When a stoichiometric complex of the modified oligonucleotide and the LCP was formed (LCP/A-1-Alexa complex), a very weak fluorescent signal was seen, indicating no or low FRET. However, when as few as 30 copies of the complementary oligonucleotide (B-1) match were added to the solution containing 10^{10} copies of the LCP/A-1-Alexa complex, the fluorescent signal became very strong. The strength of the signal attributed to a fast and efficient energy transfer from several copies of the LCP/A-1-Alexa to the LCP/A-1-Alexa/B1 complex [53]. They were able to go down to a detection limit of 5 or 18 zM depending on the experimental setup. Finally, they showed the specificity of the system by detecting five copies of a wild-type 15-mer oligonucleotide in 3-mL solution, whereas a one mismatch mutant was not detectable due to misalignment of the LCP and the Alexa Flour 546 probe.

Another similar system for detection of dsDNA and mutations in the DNA sequence was developed by Nilsson and Inganäs in 2003 [6]. The detection scheme had the same basic principle as the one originally described by Leclerc [13], although their system operated under physiological conditions without any heating. They used a zwitterionic LCP (Fig. 4e) that, free in solution, had a fluorescent peak at 540 nm and a shoulder at longer wavelength, indicating stacking of the LCP. When ssDNA was added, the LCP was red-shifted and the intensity at 540 nm was lowered as a result of planarization of the LCP backbone and increased aggregation of the LCP chains. When a complementary DNA strand was added, the LCP was blue-shifted as the helix formation induced by hybridization into dsDNA forced the LCP into a twisted conformation, and the stacking of the thiophene rings was reduced. By calculating the ratio of the intensity of the emitted light at distinct wavelengths, 540 and 585 nm (540/585 nm) and 540 and 670 nm (540/670 nm), they could detect a single base-pair mismatch in the complementary sequence at nM concentrations within 5 min. For the scheme of detection to be easy to use and to be able to assay a large number DNA sequences, they created a microarray DNA chip using soft lithography, and with this, they were able to detect a single mismatch in the complementary DNA strand down to pM concentrations (Fig 3d). Recently, Leclerc and coworkers also implemented their FRET-based system [52] into a biochip platform, and they were able to go down to attomolar detection levels on a solid support, opening up for the development of LCP based multi-arrays for fast and simple PCR-free multitarget DNA detection [54].

LCPs for detection of conformational changes in peptides and specific proteins

Peptides and proteins are known to adopt distinct conformations depending on their primary sequence of amino acids and due to the influence of the surrounding environment. It is of great importance to study the conformational flexibility of these molecules, as a wide range of pathological conditions are associated with conformational alterations or aggregation of proteins (see the following section). The detection of folding and unfolding events of proteins and peptides can be performed using the intrinsic properties of these molecules, e.g., CD or tryptophan fluorescence. In addition, small hydrophobic fluorescent dyes selective for protein aggregates, such as amyloid, have also been reported (see below) Nevertheless, the LCP and LCO technique has proven its value especially in this area. The easy preparation, fast detection schemes, flexible backbone, and low or no photobleach tendencies have given valuable insight, foremost in the field of protein aggregation. The useful properties of LCPs as molecular tools for optical assignment of distinct peptide conformations were first demonstrated by Nilsson et al.[7, 15] when they studied the formation of a four-helix bundle motif by JR2K and JR2E, two de novo designed 42 amino acids (AA) long peptides. The JR2K peptide was positively charged from an abundance of lysine AAs, and JR2E was negatively charged as eight of the lysines had been replaced by glutamic acid. When the positively charged random coil peptide was added to a solution of LCP, the LCP adopted a non-planar conformation seen as a blue-shift and as an increase in fluorescence (from reduced stacking). Conversely, if the random coil negatively charged peptide was added, the backbone adopted a planar conformation, and aggregates were formed. If both the positive and negative peptide were mixed together, the helix formation forced the LCPs apart, and it adopted a more helical structure, seen as an optical blue-shift.

In 2004, it was also demonstrated how the conformational changes in calmodulin, induced by the complexation of Ca^{2+}, altered the optical emission from a LCP [14]. The LCP did not show any induced optical changes from Ca^{2+} alone in solution; however, calmodulin red-shifted the

emission from the LCP, and when Ca^{2+} was added to the LCP/protein solution, it was blue-shifted and the intensity increased. Additionally, it was also shown that the Ca^{2+}-activated POWT-calmodulin complex could be utilized to detect the interaction between calmodulin and calcineurin, a 77-kDa calmodulin-binding protein. The ratio of the intensity of the emitted light at 540/670 nm was altered with an increasing amount of calcineurin, and the dissociation constant (K_D) for CaM and calcineurin was estimated to be approximately 36 nM. No significant change in the ratio could be seen when the calcium-activated POWT-calmodulin complex was exposed to human serum albumin. This result suggested that the alteration of the LCP emission was due to a specific interaction between the calcium activated calmodulin and calcineurin [14].

A similar approach for detection of a specific protein has also been shown by the Leclerc lab [55]. In this case, they utilized their system for recognition of structural changes in oligonucleotides by mixing their positively charged LCP and a ssDNA aptamer, designed to be specific for human α-thrombin in the presence of potassium. In a solution of thrombin and potassium, the thrombin aptamer, free in solution, is in a random coil state and adopts a unique quadruplex structure visualized by the LCP. The system was able to detect concentrations of thrombin as low as aM.

LCPs as specific ligands for protein aggregate

The formation of highly ordered aggregates of intra or extracellular proteins, so-called amyloid, underlies a wide range of diseases including neurodegenerative conditions such as prion, Parkinson's, Huntington's, and Alzheimer's (AD) diseases. From a biophysical perspective, the protein aggregates consist of fibrils with a diameter of 7–10 nm, and structural details of the fibril morphology can be visualized by transmission electron microscopy (TEM) or atomic force microscopy [56, 57]. Structural studies of amyloid have shown that the protein or peptide molecules are arranged so that the polypeptide chain forms β strands that run perpendicular to the long axis of the fibril, and it seems that many amyloid fibrils share a similar core structure independent of the amino acid sequence of the peptides building up the fibril. Hence, most peptides form comparable aggregated β-sheet-rich fibrillar assemblies, although heterogenic structures for specific types of fibrills can be observed as the alignment of adjacent strands, and the separation of the sheets might be slightly different.

The distinct repetitive β-sheet structure of amyloid fibrils has led to the development of small hydrophobic fluorescent amyloid-specific ligands. Today, the state-of-the-art chromophores for the study of protein aggregation are Congo red (CR) and Thioflavin T (ThT), but they both suffer from limitations. CR, an aromatic sulfonated azo dye, was introduced more than 80 years ago and its gold-green birefringence under polarized light has been one of the gold standard for amyloid detection ever since [58, 59]. Although the binding of CR to protein aggregates is considered specific, the method requires good control and experience to be reliable [60]. The specificity of CR binding to in vitro amyloid fibrils has, however, been questioned [61] when it was demonstrated that Congo red binds to native, partially folded conformations and amyloid fibrils of several proteins. Furthermore, not all protein aggregates are shown to be congophilic, e.g., show gold-green birefringence. ThT is another small molecule well established for use in analysis of aggregated proteins, especially for characterization of in vitro generated amyloid fibrils [62, 63]. Upon binding, ThT increases its fluorescence 100-fold depending on the protein it interacts with [64]. ThT is a blue-green-emissive dye, causing interference with autofluorescence from tissue, which is a recurring problem. Both ThT and CR are small-stiff molecules; therefore, they cannot be used to distinguish aggregates of different AA sequence or morphology within a sample. On the basis of the affinity of CR and ThT, several compounds have been synthesized to increase affinity and contrast and remove metabolic and toxic liabilities for in vivo applications as well as increasing blood–brain barrier (BBB) permeability [65–68].

Within diagnostics and pathological studies of protein aggregates associated with diseases, antibodies are the preferred technique for visualizing the amyloid. However, the shape-shifting nature of proteins or peptides when being converted to amyloid makes it hard to specifically identify amyloid with antibodies. For instance, it is hard to separate the aggregated form of the protein from the native protein as most antibodies recognize a specific sequence of a distinct protein independently of the fold of the protein. It is also commonly known that in most diseases, like AD and prionoses, a collection of different protein aggregates, such as oligomeric species and heterogeneous protein aggregates, are associated with the disease and that they occasionally appear in different regions of the diseased organ [69–74]. Similarly to CR and ThT, conventional antibodies cannot distinguish protein aggregates having different morphologies. However, conformational antibodies specific for a diversity of aggregated states of proteins, including soluble amyloid oligomers, fibrillar oligomers, or amyloid fibrils, have recently been reported [75–78]. Such conformationally specific antibodies might aid in clinical diagnostics of amyloidoses and for studying the underlying molecular and pathological events of these diseases.

In 2005, Konradsson [16] and Inganäs [16, 79] with coworkers described how two different LCPs, one anionic [79] and one zwitterionic [16], could be used for the detection of fibrillated bovine insulin and chicken lysozyme

in vitro. Fibrillated insulin is not involved in any known human disease mechanisms; nonetheless, vast amounts of insulin are produced each year as medical treatment for diabetes patients, and a reliable and fast technique to monitor aggregation of insulin during production is of great importance. Although it is rare to observe iatrogenic (i.e., treatment-induced) protein aggregates due to administration of peptide pharmaceuticals, the therapeutic effect of the peptide drug becomes limited if the peptide has been converted into amyloid fibrils. These first studies [16, 79] showed that LCPs could be utilized for distinguishing native and fibrillated proteins in vitro. Clearly, the LCPs showed a distinct spectral signature when bound to amyloid fibrils and by plotting the ratio of the intensity of the emitted light at specific wavelengths, the kinetics of amyloid fibrillation could be followed. However, the specificity of the LCPs in more complex media was yet to be demonstrated. Was it possible to, in a complex solution or preferably in tissue, stain protein aggregates without unspecific binding and background emission becoming an unsurpassable obstacle?

In 2006, Nilsson and Hammarström stained islet amyloid in pancreas ex vivo on tissue slides with three LCPs, one anionic (Fig. 4h), one cationic (Fig. 4a), and one zwitterinonic (Fig. 4f) [80]. Initially, the competition from surrounding tissue prevented detection of amyloid deposits; however, modifications of the staining protocol from physiological to more severe conditions (pH10 or pH2.5) revealed clear patterns of amyloid deposits in the expected regions. The colocalization of CR and LCP staining on consecutive slides verified that it indeed was amyloid that was stained by the LCPs. The LCP staining was also positive for amyloid in liver, kidney, and muscle tissue from intestine. Moreover, brain tissue from patients with dementia was stained with the anionic LCP, polythiopheneacetic acid (PTAA, Fig. 4h). The LCP revealed in more detail compared to CR small amyloid entities, vascular and intracellular plaques, and more importantly, these different amyloid entities could be differentiated optically. The strength of the LCP staining technique was further demonstrated in 2007 [18] by Hammarström and coworkers; the brains of a transgenic mouse model harboring the Swedish mutations K670N/M671L in the amyloid-β precursor protein APP gene (tg-APP_{Swe}) were studied. For this study, two new LCPs were prepared, one zwitterionic (Fig. 4c) and one cationic (Fig. 4b). In total, four different LCPs were used (Fig. 4b, c, f, and h), two of the LCPs (Fig. 4f and h) were polymerized from a thiophene monomer, and two were polymerized from a thiophene trimer (Fig. 4b and c). The study revealed distinct fluorometric differences especially from the zwitterionic LCP. The LCP was able to reveal small islets of compact microplaques, in a mouse of 8 months age; as seen in Fig. 5b, the plaques themselves are barely visible at a magnification that with ease reveals an abundance of plaques in a mouse of 18 months age (Fig. 5a). The plaques fluoresce intensely in orange as a result of the tight LCP packing induced by the plaques. Moreover, in a mouse of 18 months age, the LCP reveal a greenish core with an orange exterior (Fig. 5c–e). It was concluded that a likely mechanism for this difference in the density of the plaques originated from a diffuse core where the extruding branches formed are more densely packed, although it was noted that at the time, they were not able to rule out the opposite mechanism, where small plaques branch out and a diffusely packed core plaque was formed where these branches meet. The results from the study validated previously reported data [81].

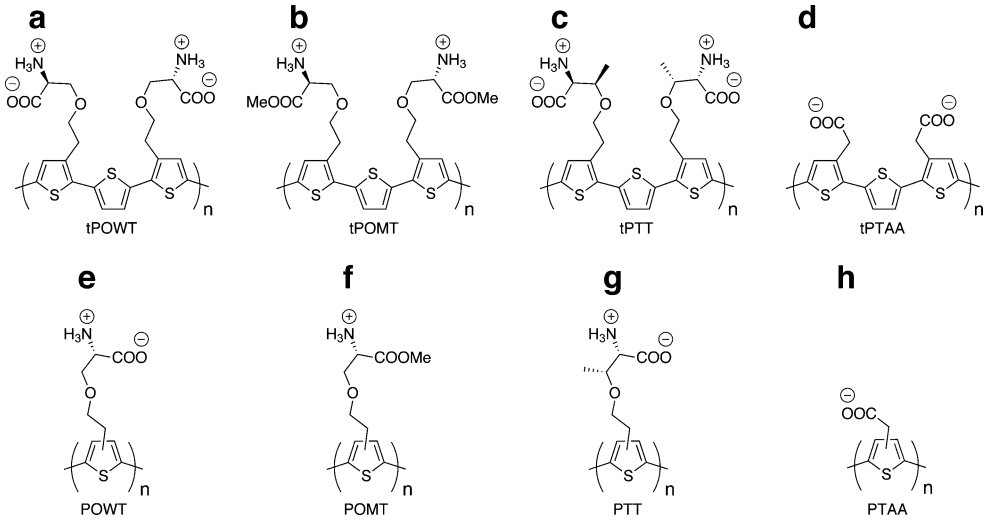

Fig. 4 **a**–**d** Trimer-based LCPs; **e**–**h** Monomer-based LCPs; Zwitterionic (**a**, **c**, **e,** and **g**), cationic (**b** and **f**), anionic (**d** and **h**)

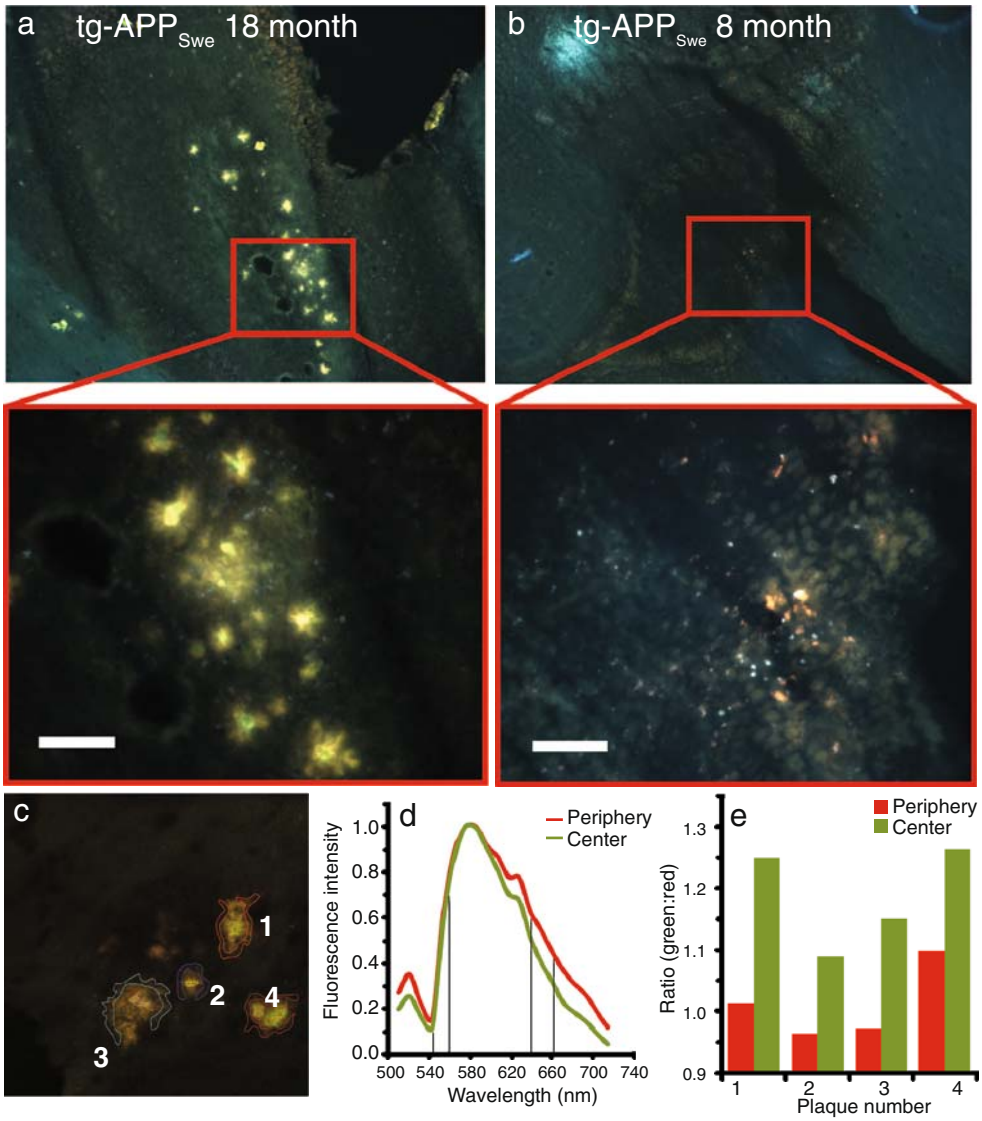

Fig. 5 **a** Histological staining of the hippocampus of an 18-month tg-APPSwe mouse with tPTT (Fig. 4c). **b** Histological staining of the hippocampus of an 8-month tg-APPSwe mouse with tPTT. The *scale bars* indicate 50 μm. **c** Confocal microscope image of four compact plaques with diffuse exterior in the cerebral cortex, where regions of the periphery and center were selected for spectral analysis as indicated with *colored lines*. **d** Normalized fluorescence spectra from the periphery and center of plaque 1 indicated in the *left panel*. The green and red spectral components are indicated. **e** Bar plot of the ratio of the fluorescence intensity of the green component and the red component of the spectra from the individual plaques 1–4 in the *left panel*. Subpanels **d** and **e** are reprinted in part with permission from American Chemical Society, *ACS Chemical Biology*, ©2007 [18]

In a study performed by Åslund et al. [17], the binding preference of LCPs with protein aggregates in vitro was evaluated. From a library of eight different LCPs, four monomer-based (Fig. 4e–h) and four trimer-based LCPs (Fig. 4a–d), important characteristics for the LCP/protein aggregate binding event were pinpointed. Each monomer-based LCP had a corresponding trimer-based LCP, with the same side chain functionality but with one out of three side chains removed. They concluded that the trimer-based LCPs were more efficient in revealing the LCP/protein aggregate interaction compared to their monomer-based counterparts, as trimer-based LCPs, to a greater extent showed larger changes in quantum efficiency and bigger spectral shifts when bound to the aggregated form of the protein. These effects are most likely due to an enhanced exposure of the hydrophobic thiophene backbone. The exposure of the backbone was brought about by the polymerization of a thiophene trimer-block, with no substituent on the center thiophene (Fig. 2h), whereas the corresponding, more steric monomer-based LCPs were substituted on every thiophene. A variety of studies suggest that amyloid-specific dyes bind in a thin hydrophobic groove along the long axis of the amyloid fibril, and recently, a similar mechanism of binding was suggested for the anionic LCP, PTAA [82, 83]. Presumably all LCOs and LCPs used for protein aggregate studies have an analogous binding to protein aggregates. Appropriate functionalization of the LCOs/LCPs for TEM and solid-state NMR evaluation of the probes bound to protein aggregates may shed more light on the mechanism of interaction between LCO/LCP and protein aggregates.

More recently, Sigurdson, Nilsson, and Aguzzi et al. applied the amyloid-staining protocol for LCPs on samples containing prion aggregates [84]. This work verified the ability of using LCPs to distinguish distinct protein aggregates arising from the same protein, as protein

aggregates associated with distinct prion strains could be separated by LCPs. Captivatingly, upon staining of formalin-fixed tissue samples with one negatively charged LCP(−) (Fig. 4h), one positively charged LCP(+) (Fig. 3b), and PrP-specific antibody SAF84, they were able to discriminate between four different mouse-adapted strains of prions (Fig. 6a) (chronic wasting disease (CWD), bovine spongiform encephalopathy (BSE), natural sheep scrapie (NS), and mouse-adapted Rocky Mountain Laboratory scrapie prions (RML)). Mouse-adapted CWD was seen with both LCPs, but NS was only seen by LCP(−), and RML was only seen by LCP(+). BSE was not seen with any of the LCPs. The different staining properties of the LCPs they pointed out were either due to tertiary and quaternary differences in the PrP aggregates or differences in the exterior decoration of the aggregates, e.g., glycosylation patterns. Formalin fixation, they pointed out, cross links the tissue and the protein deposits, and some of the native information of the deposits are thereby lost. Therefore, they prepared frozen brain sections fixed in ethanol, and these experiments revealed congophilic protein aggregates for some of the mouse-adapted prion strains. Fascinatingly, these types of congophilic aggregates could be separated thanks to the optical fingerprint obtained from LCP(−). This was shown in a correlation diagram and by plotting the ratio 532/639 nm against the ratio 532/excitation max; strains such as mouse-adapted CWD, sheep scrapie and BSE were easily separated in the 2D diagram (Fig. 6b). It was also shown that the optical fingerprint observed for LCP (−) bound to protein deposits related to distinct prion strains most likely occurred due to a structural variance of the protein deposits. By taking recombinant mouse prion protein (mPrP) and converting it into two different types of amyloid fibrils, Sigurdson et al. were able to show that the emission profile of PTAA could be used to distinguish these two fibril preparations (Fig. 6c) [84]. As these two preparations of fibrils were chemically identical, having the same protein (mPrP), the spectral differences seen for LCP(−) were most likely due to structural differences between the fibrils. Similar observations have also been made using Aβ 1–42 amyloid fibrils grown under different conditions in vitro [18] and amyloid fibrils built from reduced or intact bovine insulin [85]. In these studies, the zwitterionic LCP, tPTT (Fig. 4c) [18], or the cationic LCP, POMT (Fig. 4f) [85], were used, showing that distinct LCPs can be used to differentiate protein aggregates of diverse origin. Hence, LCPs have so far been shown to provide indirect structural insights regarding the morphology of individual protein deposits, and these findings may be of great value, as phenomena similar to those occurring in prion strains may be much more frequent than is now appreciated and may extend to additional proteinopathies.

In 2009, Sigurdson and coworkers yet again used the staining technique in the study of a two-point mutation in the PrP codon reading frame [86]. The mutation locks a normally flexible loop in the PrP protein into a fixed position and, hence, is referred to as the rigid loop mutation (RL). RL induces neurological disease in mice with no exceptions; the reference *tga20* mouse did not, even at doubled concentration of the PrP protein compared to the RL mouse, develop spontaneous PrP plaques. The toxicity of the mutation was consequently attributed to the loop

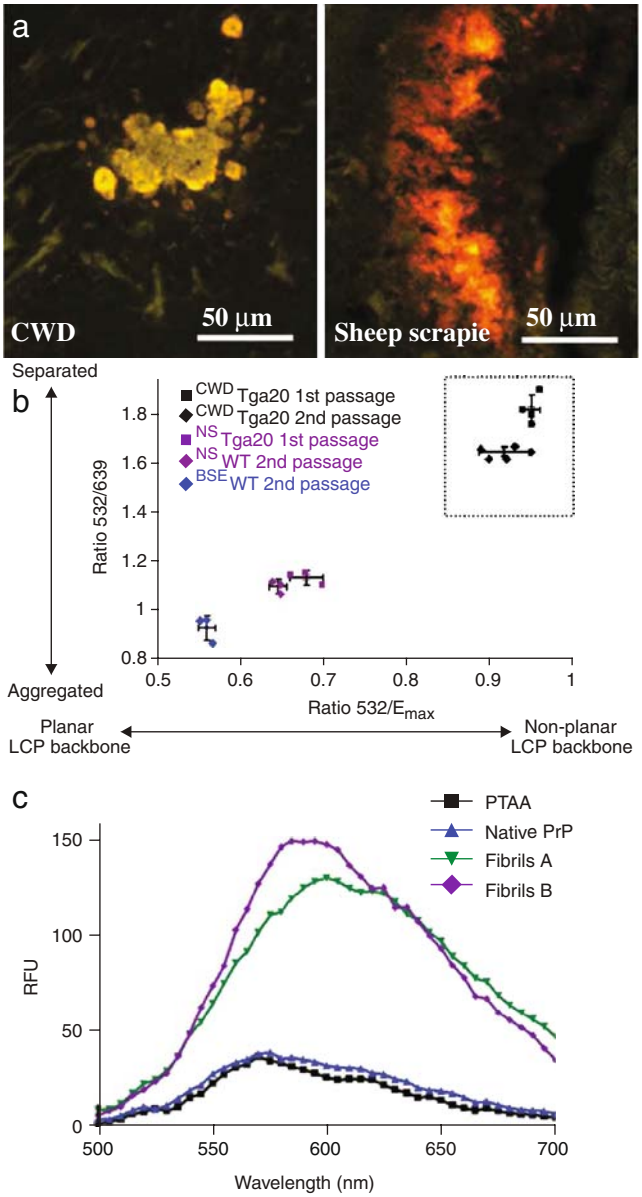

Fig. 6 **a** Sections of CWD and sheep scrapie stained with LCP(-). **b** Ratio plots of the ratio 532 nm/Emax vs. the ratio of 532/639 nm distinguishing CWD, BSE and sheep scrapie. **c** Spectras of LCP(-) (PTAA), native PrP, and recombinant PrP. Fibrillation of preparation A are started from natively folded recPrP, and fibrillation of preparation B are started from denatured recPrP. Reprinted by permission from Macmillan Publishers Ltd: *Nature Methods* [84], ©(2007)

being in a fixed position, propitious for aggregation. The LCP technique was used for specific spectral assignment of the protein deposits, and the aggregates occurring in the de novo-generated prion strain were distinguished from the previously reported prion strains [84]. Interestingly, the prion deposits were not stained by any of the conventional amyloid ligands, ThT, or Congo red, indicating that LCPs could be used to identify a subset of protein deposits normally undetectable by conventional methods [86].

Future challenges for LCOs and LCPs

For the study of protein aggregation diseases, in vivo imaging is the next natural step to take. To prove that the probes are nontoxic and that they can be injected for subsequent analysis of the desired organ are two major obstacles to surpass. For studies in organs other than the brain, the size of the probe is not crucial, but if the probe is to pass the BBB, it has to be relatively small, preferably <600 D; this means that the well-defined smaller LCOs probably are more suitable than the LCPs. Furthermore, we foresee that LCOs will be the dominating optical probe for in vivo studies of protein aggregates due to their well-defined optical characteristics but foremost for the ease of which they can be functionalized. Ongoing work in our own facilities is directed mainly towards LCOs for in vivo studies. The availability of LCOs that cross the BBB opens possibilities for several different studies, e.g., indirect protein deposit age determination, discrimination of different morphologies of plaques, and live imaging of the plaques. Several of the LCPs discussed in this review have already been proven to be two-photon active [85, 87]. Two-photon activity means that the LCPs/LCOs can be excited with light in the near-IR region (e.g., 886 nm). At this wavelength, the energy of the photons of excitation is approximately half the normal energy; to simplify, two photons are needed to excite the electron. Near-IR has fairly low absorbance from soft tissue in living matter and can penetrate the tissue up to 100 μM. This feature will make live imaging of plaques in animal models possible of the kind described by Jucker and coworkers [88] and Bacskai and coworkers [89].

Recently, it has been suggested that maybe the time has come for the LCOs/LCPs to go back to their initially intended use and, by making proper modifications, build electronic devices [90]. The stable and structurally defined amyloid fibrils can be used as a template for making well-defined nanowires on which conjugated polymers can be symmetrically aligned. Hence, amyloid fibrils might offer an attractive avenue for development of functional nano-devices. The Inganäs and Konradsson group has shown that both fluorescent and conducting conjugated polymers can be used to decorate amyloid fibrils or be incorporated into amyloid fibrils, opening up a way for controlling the alignment of conjugated polymers in organic electronic devices [91]. Recently, Li et al. used triblock peptide copolymers and a LCP (Fig. 4g) to build nanotapes that they propose can be used in nano-electronic devices [92]. Hence, the future for implementing organic materials within biology appears to be as bright as ever before.

In conclusion, LCOs and LCPs have shown great potential as light-emitting probes in a variety of biological systems. The straightforward use, robustness, sensitivity, and information they provide suggest that these molecular agents may be an important research tool, foremost in the study of protein aggregation diseases. LCPs and LCOs are already at use in labs ranging from medicine to chemistry and physics, indicating that they have found a practical use within the field of chemical biology.

Acknowledgements Our work is supported by the Swedish Foundation for Strategic Research (as a grant to the research consortium OBOE, K.P.R.N, P.K., and A.Å and as a repatriation grant, Ingvar Carlsson award, K.P.R.N.) and the Knut and Alice Wallenberg foundation (K.P.R.N.). A generous gift from Astrid and Georg Olsson is also gratefully acknowledged and the Swedish research foundation (P.K). A.Å is enrolled in the doctoral program Forum Scientum.

References

1. Andersson M, Ekeblad PO, Hjertberg T, Wennerström O, Ingenäs O (1991) Polythiophene with a free amino acid side chain. Polym Commun (Guildf) 32(18):546–548
2. Nilsson KPR, Andersson MR, Inganäs O (2002) Conformational transitions of a free amino-acid-functionalized polythiophene induced by different buffer systems. J Phys Condens Matter 14 (42):10011–10020
3. Charych DH, Nagy JO, Spevak W, Bednarski MD (1993) Direct colorimetric detection of a receptor-ligand interaction by a polymerized bilayer assembly. Science 261(5121):585–588
4. Ewbank PC, Nuding G, Suenaga H, McCullough RD, Shinkai S (2001) Amine functionalized polythiophenes: synthesis and formation of chiral, ordered structures on DNA substrates. Tetrahedron Lett 42(2):155–157
5. Barbarella G, Zambianchi M, Pudova O, Paladini V, Ventola A, Cipriani F, Gigli G, Cingolani R, Citro G (2001) Oligothiophene lsothiocyanates as a new class of fluorescent markers for biopolymers. J Am Chem Soc 123(47):11600–11607
6. Nilsson KPR, Inganäs O (2003) Chip and solution detection of DNA hybridization using a luminescent zwitterionic polythiophene derivative. Nat Mater 2(6):419–U10
7. Nilsson KPR, Rydberg J, Baltzer L, Inganäs O (2003) Self-assembly of synthetic peptides control conformation and optical properties of a zwitterionic polythiophene derivative. Proc Natl Acad Sci U S A 100(18):10170–10174
8. Eberhard O (1894) Chem Ber 27:2919
9. Lin JWP, Dudek LP (1980) Synthesis and properties of POLY(2,5-THIENYLENE). J Polym Sci A-1 Polym Chem 18(9):2869–2873
10. Takakazu Yamamoto KSAY (1980) Preparation of thermostable and electric-conducting poly(2,5-thienylene). J Polym Sci Polym Lett Ed 18(1):9–12

11. Yoshino K, Hayashi S, Sugimoto R-I (1984) Preparation and properties of conducting heterocyclic polymer films by chemical method. Jpn J Appl Phys Lett 23(12):899–900
12. Baek MG, Stevens RC, Charych DH (2000) Design and synthesis of novel glycopolythiophene assemblies for colorimetric detection of influenza virus and *E. coli*. Bioconjug Chem 11(6):777–788
13. Ho HA, Boissinot M, Bergeron MG, Corbeil G, Dore K, Boudreau D, Leclerc M (2002) Colorimetric and fluorometric detection of nucleic acids using cationic polythiophene derivatives. Angew Chem Int Edit 41(9):1548–1551
14. Nilsson KPR, Inganäs O (2004) Optical emission of a conjugated polyelectrolyte: calcium-induced conformational changes in calmodulin and calmodulin–calcineurin interactions. Macromolecules 37(24):9109–9113
15. Nilsson KPR, Rydberg J, Baltzer L, Inganäs O (2004) Twisting macromolecular chains: self-assembly of a chiral supermolecule from nonchiral polythiophene polyanions and random-coil synthetic peptides. Proc Natl Acad Sci U S A 101(31):11197–11202
16. Herland A, Nilsson KPR, Olsson JDM, Hammarström P, Konradsson P, Inganäs O (2005) Synthesis of a regioregular zwitterionic conjugated oligoelectrolyte, usable as an optical probe for detection of amyloid fibril formation at acidic pH. J Am Chem Soc 127(7):2317–2323
17. Åslund A, Herland A, Hammarström P, Nilsson KP, Jonsson BH, Inganäs O, Konradsson P (2007) Studies of luminescent conjugated polythiophene derivatives: enhanced spectral discrimination of protein conformational States. Bioconjug Chem 18(6):1860–1868
18. Nilsson KPR, Åslund A, Berg I, Nyström S, Konradsson P, Herland A, Inganäs O, Stabo-Eeg F, Lindgren M, Westermark GT, Lannfelt L, Nilsson LN, Hammarström P (2007) Imaging distinct conformational states of amyloid-beta fibrils in Alzheimer's disease using novel luminescent probes. ACS Chem Biol 2 (8):553–560
19. Chayer M, Faïd K, Leclerc M (1997) Highly conducting water-soluble polythiophene derivatives. Chem Mater 9(12):2902–2905
20. Karlsson RH, Herland A, Mahiar H, Wigenius JA, Åslund A, Inganäs O, Konradsson P (2009) Iron-catalyzed polymerization of alkoxysulfonate-functionalized 3, 4-ethylenedioxythiophene gives water-soluble poly(3,4-ethylenedioxythiophene) of high conductivity. Chem Mater 21(9):1815–1821. doi:10.1021/cm801512r
21. McCarley TD, Noble, DuBois CJ, McCarley RL (2001) MALDI-MS evaluation of poly(3-hexylthiophene) synthesized by chemical oxidation with FeCl3. Macromolecules 34(23):7999–8004
22. Nilsson KPR, Olsson JDM, Konradsson P, Inganäs O (2004) Enantiomeric substituents determine the chirality of luminescent conjugated polythiophenes. Macromolecules 37(17):6316–6321
23. Pomerantz M, Tseng JJ, Zhu H, Sproull SJ, Reynolds JR, Uitz R, Arnott HJ, Haider MI (1991) Processable polymers and copolymers of 3-alkylthiophenes and their blends. Synth Met 41(3):825–830
24. Yue S, Berry GC, McCullough RD (1996) Intermolecular association and supramolecular organization in dilute solution. 1. Regioregular poly(3-dodecylthiophene). Macromolecules 29 (3):933–939
25. Jayakannan M, van Dongen JLJ, Janssen RAJ (2001) Mechanistic aspects of the Suzuki polycondensation of thiophenebisboronic derivatives and diiodobenzenes analyzed by MALDI-TOF mass spectrometry. Macromolecules 34(16):5386–5393
26. McCullough RD, Lowe RD (1992) Enhanced electrical-conductivity in regioselectively synthesized poly(3-alkylthiophenes). J Chem Soc Chem Commun 1:70–72
27. Maior RMS, Hinkelmann K, Eckert H, Wudl F (1990) Synthesis and characterization of 2 regiochemically defined Poly(Dialkylbithiophenes)—a comparative-study. Macromolecules 23(5):1268–1279
28. McCullough RD (1998) The chemistry of conducting polythiophenes. Adv Mater 10(2):93–116
29. Osaka I, McCullough RD (2008) Advances in molecular design and synthesis of regioregular polythiophenes. Acc Chem Res 41 (9):1202–1214
30. Stille J (1986) The Palladium-catalyzed cross-coupling reactions of organotin reagents with organic electrophiles [New Synthetic Methods (58)]. Angew Chem Int Ed Engl 25(6):508–524
31. Miyaura N, Yamada K, Suzuki A (1979) A new stereospecific cross-coupling by the palladium-catalyzed reaction of 1-alkenylboranes with 1-alkenyl or 1-alkynyl halides. Tetrahedron Lett 20(36):3437–3440
32. Miyaura N, Suzuki A (1979) Stereoselective synthesis of arylated (E)-alkenes by the reaction of alk-1-enylboranes with aryl halides in the presence of palladium catalyst. J Chem Soc Chem Commun 19:866–867
33. Farina V, Krishnan B (1991) Large rate accelerations in the stille reaction with Tri-2-Furylphosphine and Triphenylarsine as palladium ligands - mechanistic and synthetic Implications. J Am Chem Soc 113(25):9585–9595
34. Herrmann WA, Elison M, Fischer J, Köcher C, Artus GRJ (1995) Metal complexes of N-heterocyclic carbenes—a new structural principle for catalysts in homogeneous catalysis. Angew Chem Int Ed Engl 34(21):2371–2374
35. Kantchev EAB, O'Brien CJ, Organ MG (2007) Palladium complexes of N-heterocyclic carbenes as catalysts for cross-coupling reactions - A synthetic chemist's perspective. Angew Chem Int Ed Engl 46(16):2768–2813
36. Martina S, Enkelman V, Schlueter AD, Wegner G (1991) Polypyrrole: towards the development of a chemical synthesis. Synth Met 41(1–2):403–406
37. Melucci M, Barbarella G, Sotgiu G (2002) Solvent-free, microwave-assisted synthesis of thiophene oligomers via Suzuki coupling. J Org Chem 67(25):8877–8884
38. Kirschbaum T, Azumi R, Mena-Osteritz E, Bauerle P (1999) Synthesis and characterization of structurally defined head-to-tail coupled oligo(3-alkylthiophenes). New J Chem 23(2):241–250
39. Briehn CA, Kirschbaum T, Bauerle P (2000) Polymer-supported synthesis of regioregular head-to-tail-coupled Oligo (3-arylthiophene)s utilizing a traceless silyl linker. J Org Chem 65(2):352–359
40. Kirschbaum T, Briehn CA, Bauerle P (2000) Efficient solid-phase synthesis of regioregular head-to-tail-coupled oligo(3-alkylthiophene)s up to a dodecamer. J Chem Soc Perkin Trans 1 8:1211–1216
41. Cremer J, Mena-Osteritz E, Pschierer NG, Mullen K, Bauerle P (2005) Dye-functionalized head-to-tail coupled oligo(3-hexylthiophenes)-perylene-oligothiophene dyads for photovoltaic applications. Org Biomol Chem 3(6):985–995
42. Villemin D, Caillot F (2001) Microwave mediated palladium-catalysed reactions on potassium fluoride/alumina without use of solvent. Tetrahedron Lett 42(4):639–642
43. Organ MG, Avola S, Dubovyk I, Hadei N, Kantchev EAB, O'Brien CJ, Valente C (2006) A user-friendly, all-purpose Pd-NHC (NHC=N-heterocyclic carbene) precatalyst for the Negishi reaction: a step towards a universal cross-coupling catalyst. Chemistry 12(18):4749–4755
44. Rosivatz E (2008) Imaging the boundaries—innovative tools for microscopy of living cells and real-time imaging. J Chem Biol 1(1):3–15
45. Leclerc M (1999) Optical and electrochemical transducers based on functionalized conjugated polymers. Adv Mater 11(18):1491–1498
46. Zhou Q, Swager TM (1995) Methodology for enhancing the sensitivity of fluorescent chemosensors - energy migration in conjugated polymers. J Am Chem Soc 117(26):7017–7018
47. Zhou Q, Swager TM (1995) Fluorescent chemosensors based on energy migration in conjugated polymers: The molecular wire approach to increased sensitivity. J Am Chem Soc 117(50): 12593–12602

48. Wang J, Wang DL, Miller EK, Moses D, Bazan GC, Heeger AJ (2000) Photoluminescence of water-soluble conjugated polymers: Origin of enhanced quenching by charge transfer. Macromolecules 33(14):5153–5158
49. Harrison BS, Ramey MB, Reynolds JR, Schanze KS (2000) Amplified fluorescence quenching in a poly(p-phenylene)-based cationic polyelectrolyte. J Am Chem Soc 122(35):8561–8562
50. Jones RM, Bergstedt TS, McBranch DW, Whitten DG (2001) Tuning of superquenching in layered and mixed fluorescent polyelectrolytes. J Am Chem Soc 123(27):6726–6727
51. Ho HA, Najari A, Leclerc M (2008) Optical Detection of DNA and Proteins with Cationic Polythiophenes. Acc. Chem. Res 41(2):168–178
52. Ho HA, DorÈ K, Boissinot M, Bergeron MG, Tanguay RM, Boudreau D, Leclerc M (2005) Direct molecular detection of nucleic acids by fluorescence signal amplification. J Am Chem Soc 127(36):12673–12676
53. Doré K, Leclerc M, Boudreau D (2006) Investigation of a fluorescence signal amplification mechanism used for the direct molecular detection of nucleic acids. J Fluoresc 16(2):259–265
54. Najari A, Ho HA, Gravel JF, Nobert P, Boudreau D, Leclerc M (2006) Reagentless ultrasensitive specific DNA array detection based on responsive polymeric biochips. Anal Chem 78(22):7896–7899
55. Ho HA, Leclerc M (2004) Optical sensors based on hybrid aptamer/conjugated polymer complexes. J Am Chem Soc 126 (5):1384–1387
56. Serpell LC, Sunde M, Blake CC (1997) The molecular basis of amyloidosis. Cell Mol Life Sci 53(11–12):871–887
57. Harper JD, Lieber CM, Lansbury PT Jr (1997) Atomic force microscopic imaging of seeded fibril formation and fibril branching by the Alzheimer's disease amyloid-beta protein. Chem Biol 4 (12):951–959
58. Bennhold H (1922) Eine specifische Amyloidfärbung mit Kongorot. Műnchener Med. Wochenschrift 44:1537–1537
59. Divry P (1927) Etude histochimique des plaques seniles. J. Belge Neurol Psychiatry 27:643–657
60. Westermark GT, Johnson KH, Westermark P (1999) Staining methods for identification of amyloid in tissue. Methods Enzymol 309:3–25
61. Khurana R, Uversky VN, Nielsen L, Fink AL (2001) Is Congo red an amyloid-specific dye? J Biol Chem 276(25):22715–22721
62. Naiki H, Higuchi K, Hosokawa M, Takeda T (1989) Fluorometric determination of amyloid fibrils in vitro using the fluorescent dye, thioflavin T1. Anal Biochem 177(2):244–249
63. LeVine H 3rd (1993) Thioflavine T interaction with synthetic Alzheimer's disease beta-amyloid peptides: detection of amyloid aggregation in solution. Protein Sci 2(3):404–410
64. Voropai ES, Samtsov MP, Kaplevskii KN, Maskevich AA, Stepuro VI, Povarova OI, Kuznetsova IM, Turoverov KK, Fink AL, Uverskii VN (2003) Spectral properties of thioflavin T and its complexes with amyloid fibrils. J Appl Spectrosc 70 (6):868–874
65. Crystal AS, Giasson BI, Crowe A, Kung MP, Zhuang ZP, Trojanowski JQ, Lee VM (2003) A comparison of amyloid fibrillogenesis using the novel fluorescent compound K114. J Neurochem 86(6):1359–1368
66. LeVine H 3rd (2005) Mechanism of A beta(1–40) fibril-induced fluorescence of (trans, trans)-1-bromo-2, 5-bis(4-hydroxystyryl) benzene (K114). Biochemistry 44(48):15937–15943
67. Styren SD, Hamilton RL, Styren GC, Klunk WE (2000) X-34, a fluorescent derivative of Congo red: a novel histochemical stain for Alzheimer's disease pathology. J Histochem Cytochem 48 (9):1223–1232
68. Nesterov EE, Skoch J, Hyman BT, Klunk WE, Bacskai BJ, Swager TM (2005) In vivo optical imaging of amyloid aggregates in brain: design of fluorescent markers. Angew Chem Int Edit 44 (34):5452–5456
69. Fraser H, Dickinson AG (1968) The sequential development of the brain lesion of scrapie in three strains of mice. J Comp Pathol 78(3):301–311
70. Fraser H, Dickinson AG (1973) Scrapie in mice. Agent-strain differences in the distribution and intensity of grey matter vacuolation. J Comp Pathol 83(1):29–40
71. Bruce ME, McBride PA, Farquhar CF (1989) Precise targeting of the pathology of the sialoglycoprotein, PrP, and vacuolar degeneration in mouse scrapie. Neurosci Lett 102(1):1–6
72. Bessen RA, Marsh RF (1992) Biochemical and physical properties of the prion protein from two strains of the transmissible mink encephalopathy agent. J Virol 66(4):2096–2101
73. Hill AF, Joiner S, Beck JA, Campbell TA, Dickinson A, Poulter M, Wadsworth JD, Collinge J (2006) Distinct glycoform ratios of protease resistant prion protein associated with PRNP point mutations. Brain 129(Pt 3):676–685
74. Chiti F, Dobson CM (2006) Protein misfolding, functional amyloid, and human disease. Ann Rev Biochem 75:333–366
75. Kayed R, Head E, Thompson JL, McIntire TM, Milton SC, Cotman CW, Glabe CG (2003) Common structure of soluble amyloid oligomers implies common mechanism of pathogenesis. Science 300(5618):486–489
76. Kayed R, Head E, Sarsoza F, Saing T, Cotman CW, Necula M, Margol L, Wu J, Breydo L, Thompson JL, Rasool S, Gurlo T, Butler P, Glabe CG (2007) Fibril specific, conformation dependent antibodies recognize a generic epitope common to amyloid fibrils and fibrillar oligomers that is absent in prefibrillar oligomers. Mol Neurodegener 2:18
77. Lambert MP, Velasco PT, Chang L, Viola KL, Fernandez S, Lacor PN, Khuon D, Gong Y, Bigio EH, Shaw P, De Felice FG, Krafft GA, Klein WL (2007) Monoclonal antibodies that target pathological assemblies of Abeta. J Neurochem 100(1):23–35
78. Wang XP, Zhang JH, Wang YJ, Feng Y, Zhang X, Sun XX, Li JL, Du XT, Lambert MP, Yang SG, Zhao M, Klein WL, Liu RT (2009) Conformation-dependent single-chain variable fragment antibodies specifically recognize beta-amyloid oligomers. FEBS Lett 583(3):579–584
79. Nilsson KPR, Herland A, Hammarström P, Inganäs O (2005) Conjugated polyelectrolytes: Conformation-sensitive optical probes for detection of amyloid fibril formation. Biochemistry 44(10):3718–3724
80. Nilsson KPR, Hammarström P, Ahlgren F, Herland A, Schnell EA, Lindgren M, Westermark GT, Inganäs O (2006) Conjugated polyelectrolytes - Conformation-sensitive optical probes for staining and characterization of amyloid deposits. Chembiochem 7(7):1096–1104
81. Jin LW, Claborn KA, Kurimoto M, Geday MA, Maezawa I, Sohraby F, Estrada M, Kaminksy W, Kahr B (2003) Imaging linear birefringence and dichroism in cerebral amyloid pathologies. Proc Natl Acad Sci U S A 100(26):15294–15298
82. Groenning M, Norrman M, Flink JM, van de Weert M, Bukrinsky JT, Schluckebier G, Frokjaer S (2007) Binding mode of Thioflavin T in insulin amyloid fibrils. J Struct Biol 159(3):483–497
83. Herland A, Bjork P, Hania PR, Scheblykin IG, Inganäs O (2007) Alignment of a conjugated polymer onto amyloid-like protein fibrils. Small 3(2):318–325
84. Sigurdson CJ, Nilsson KP, Hornemann S, Manco G, Polymenidou M, Schwarz P, Leclerc M, Hammarström P, Wuthrich K, Aguzzi A (2007) Prion strain discrimination using luminescent conjugated polymers. Nat Methods 4(12):1023–1030
85. Stabo-Eeg F, Lindgren M, Nilsson KPR, Inganäs O, Hammarström P (2007) Quantum efficiency and two-photon absorption cross-section of conjugated polyelectrolytes used for protein conformation measurements with applications on amyloid structures. Chem Phys 336(2–3):121–126

86. Sigurdson CJ, Nilsson KP, Hornemann S, Heikenwalder M, Manco G, Schwarz P, Ott D, Rulicke T, Liberski PP, Julius C, Falsig J, Stitz L, Wuthrich K, Aguzzi A (2009) De novo generation of a transmissible spongiform encephalopathy by mouse transgenesis. Proc Natl Acad Sci U S A 106(1):304–309
87. Nilsson KPR, Olsson JDM, Stabo-Eeg F, Lindgren M, Konradsson P, Inganäs O (2005) Chiral recognition of a synthetic peptide using enantiomeric conjugated polyelectrolytes and optical spectroscopy. Macromolecules 38(16):6813–6821
88. Bolmont T, Haiss F, Eicke D, Radde R, Mathis CA, Klunk WE, Kohsaka S, Jucker M, Calhoun ME (2008) Dynamics of the microglial/amyloid interaction indicate a role in plaque maintenance. J Neurosci 28(16):4283–4292
89. Kuchibhotla KV, Lattarulo CR, Hyman BT, Bacskai BJ (2009) Synchronous hyperactivity and intercellular calcium waves in astrocytes in alzheimer mice. Science 323(5918):1211–1215
90. Nilsson KPR, Hammarström P (2008) Luminescent conjugated polymers: illuminating the dark matters of biology and pathology. Adv Mater 20(13):2639–2645
91. Hamedi M, Herland A, Karlsson RH, Inganäs O (2008) Electrochemical devices made from conducting nanowire networks self-assembled from amyloid fibrils and alkoxysulfonate PEDOT. Nano Lett 8(6):1736–1740
92. Li F, Martens AA, Åslund A, Konradsson P, de Wolf FA, Stuart MAC, Sudholter EJR, Marcelis ATM, Leermakers FAM (2009) Formation of nanotapes by co-assembly of triblock peptide copolymers and polythiophenes in aqueous solution. Soft Matter 5:1668–1673